



OPEN ACCESS

EDITED BY

Nasrddine Youbi,
Cadi Ayyad University, Morocco

REVIEWED BY

Umar Ashraf,
Yunnan University, China
Raymond Duraiswami,
Savitribai Phule Pune University, India

*CORRESPONDENCE

Dingyong Liang,
✉ 381501713@qq.com
Zailong Hu,
✉ 272464990@qq.com

RECEIVED 17 April 2025

ACCEPTED 02 June 2025

PUBLISHED 26 June 2025

CITATION

Lin Y, Liang D, Hu Z, Yuan Q, Lv Z and Guan J
(2025) Petrogenesis and geotectonic
significance of magnesian andesite in the
Nangunyuan area, northern Hainan Island,
China.
Front. Earth Sci. 13:1613531.
doi: 10.3389/feart.2025.1613531

COPYRIGHT

© 2025 Lin, Liang, Hu, Yuan, Lv and Guan.
This is an open-access article distributed
under the terms of the [Creative Commons
Attribution License \(CC BY\)](https://creativecommons.org/licenses/by/4.0/). The use,
distribution or reproduction in other forums is
permitted, provided the original author(s) and
the copyright owner(s) are credited and that
the original publication in this journal is cited,
in accordance with accepted academic
practice. No use, distribution or reproduction
is permitted which does not comply with
these terms.

Petrogenesis and geotectonic significance of magnesian andesite in the Nangunyuan area, northern Hainan Island, China

Yihua Lin^{1,2}, Dingyong Liang^{1,2*}, Zailong Hu^{1,2*}, Qinmin Yuan^{1,2},
Zhaoying Lv^{1,2} and Jun Guan^{1,2}

¹Hainan Key Laboratory of Marine Geological Resources and Environment, Haikou, China, ²Hainan Provincial Institute of Geological Survey, Haikou, China

The Magnesian andesite discovered in the Nangunyuan area of northern Hainan Island provides an important research object for constraining the tectonic evolution process of the Paleo-Tethys Ocean in Southeast Asia. The formation age of the Magnesian andesite in the Nangunyuan area of northern Hainan Island was determined to be 251.2 ± 4.5 Ma in the late Permian by LA-ICP-MS zircon U-Pb dating. The Magnesian andesite is characterized by relatively high contents of SiO₂, CaO, and MgO, and relatively low contents of Na₂O, K₂O, and FeO. It is enriched in large ion lithophile elements and relatively depleted in high field strength elements, with obvious negative anomalies of Ta, Nb, and Ti. It has geochemical characteristics similar to those of Sanukite and belongs to island arc volcanic rocks. The Magnesian andesite may be formed by the equilibrium reaction between the mantle peridotite and the Si-rich melt from the partial melting of the subducting oceanic crust slab or sediment. It is the product of the wedge mantle source region of the Changjiang-Qionghai tectonic belt affected by the metasomatism of the subduction component. Its formation age is close to the closure time of the Paleo-Tethys Ocean, which may mark the late stage of the subduction of the Paleo-Tethys Ocean. The discovery of the late Permian Magnesian andesite in northern Hainan Island reveals the late-stage dynamics of the subduction of the Paleo-Tethys Ocean. Its magma source mixing origin reflects the complex interactions between the crust and mantle in the subduction zone. This discovery is of great scientific value for constraining the closure time of the Paleo-Tethys Ocean, understanding the formation mechanism of the Paleo-Tethys orogenic belt, and regional metallogeny.

KEYWORDS

magnesian andesite, volcanic rocks, eastern paleo-tethys ocean, sanukite, late permian

Introduction

Situated at the convergent junction of the Eurasian, Pacific, Indochina, and Philippine Sea plates, Hainan Island's geological evolution has been jointly controlled by both Paleo-Pacific and Tethyan tectonic regimes. As a "geological bridgehead" extending from mainland China to the South China Sea, this region preserves

critical evidence documenting multi-stage tectonic events including the closure of the Paleo-Asian Ocean, evolution of the Tethyan Ocean, and Pacific subduction, making it a key window for deciphering East Asian continental accretion and supercontinent cyclicity (Li et al., 2000a; Liu et al., 2021). Although previous studies established a fundamental “EW-zonation and NS-blocking” tectonic framework (Xu et al., 2001; Ding et al., 2005), significant controversies persist regarding core scientific issues such as its tectonic affinity, precise unit boundaries, spatial distribution of sutures, and final amalgamation timing (Li et al., 2002; Shen et al., 2018). Outstanding debates include whether Hainan constitutes Gondwana-derived fragments and preserves remnants of Paleo-Tethyan subduction zones, while Late Mesozoic paleomagnetic and biogeographic evidence further reveals complex rotational drift trajectories (Liu et al., 2022a; b; Wang et al., 2022; Lv et al., 2023; Wei et al., 2023; Sheir et al., 2024; Ashraf et al., 2024).

Magnesian andesites represent a distinctive magma type with diagnostic geochemical signatures and specific petrogenetic settings, serving as critical probes for deep crust-mantle interactions and plate dynamics (Dong and Santosh, 2016; Gao et al., 2022). High-Mg andesites (HMA) are typically defined by $\text{SiO}_2 > 52$ wt%, elevated MgO (> 5 wt%) with $\text{Mg}^\# > 55$, enriched Ni-Cr, and low $\text{FeO}^\text{T}/\text{MgO} (< 1)$, whereas evolved magnesian andesites (MA) may exhibit lower MgO (two to three wt%) while maintaining high $\text{Mg}^\#$ with reduced Ni-Cr contents. Deng et al. (2010) classified these rocks into HMA and MA based on SiO_2 -MgO- $\text{FeO}^\text{T}/\text{MgO}$ systematics: HMAs originate from hydrous melting of mantle wedges above subduction zones, while MAs form through interaction between slab-derived melts/fluids and overlying mantle under high thermal gradients in subduction-related environments.

Late Paleozoic volcanic rocks remain poorly exposed in Hainan, with Permian volcanism particularly understudied. Existing research has primarily focused on limited Late Paleozoic volcanic units in southern and central-western Hainan (He et al., 2016; Gou et al., 2019), leaving critical gaps in understanding the island's Permian tectonic evolution. Our recent discovery of Permian intermediate lavas in the Nangunyuan area (northern Hainan) provides new constraints through integrated LA-ICP-MS zircon U-Pb geochronology and petrochemical analyses. By characterizing these magnesian andesites' geochemical fingerprints and comparing their age spectra with regional tectono-magmatic events, this study aims to: elucidate their petrogenesis, decipher tectonic implications and establish robust geological evidence for reconstructing Hainan's Permian evolution. These findings hold significant implications for determining the closure timing of the eastern Paleo-Tethys Ocean, understanding Paleo-Tethyan orogenic mechanisms, and regional metallogeny.

Geological settings

Hainan Island is geographically separated from the South China Block by the Qiongzhou Strait and adjoins the Indochina Block through the Beibu Gulf, occupying a critical junction between the Paleo-Tethyan and Paleo-Pacific tectonic domains (Figure 1a).

The island has undergone multiple tectonic episodes including the Jinningian, Caledonian, Hercynian, Indosinian, Yanshanian, and Himalayan orogenies, resulting in dominant EW- and NE-trending structural systems with subordinate NS-oriented structures (Figure 1b) (Chao et al., 2016; Liang et al., 2018). The EW-trending tectonic framework comprises four major belts from north to south: the Wangwu-Wenchang, Changjiang-Qionghai, Jianfeng-Diaoluo, and Jiusuo-Lingshu tectonic zones (Liang et al., 2018). NE-trending structures are principally represented by the Gezhen and Baisha faults.

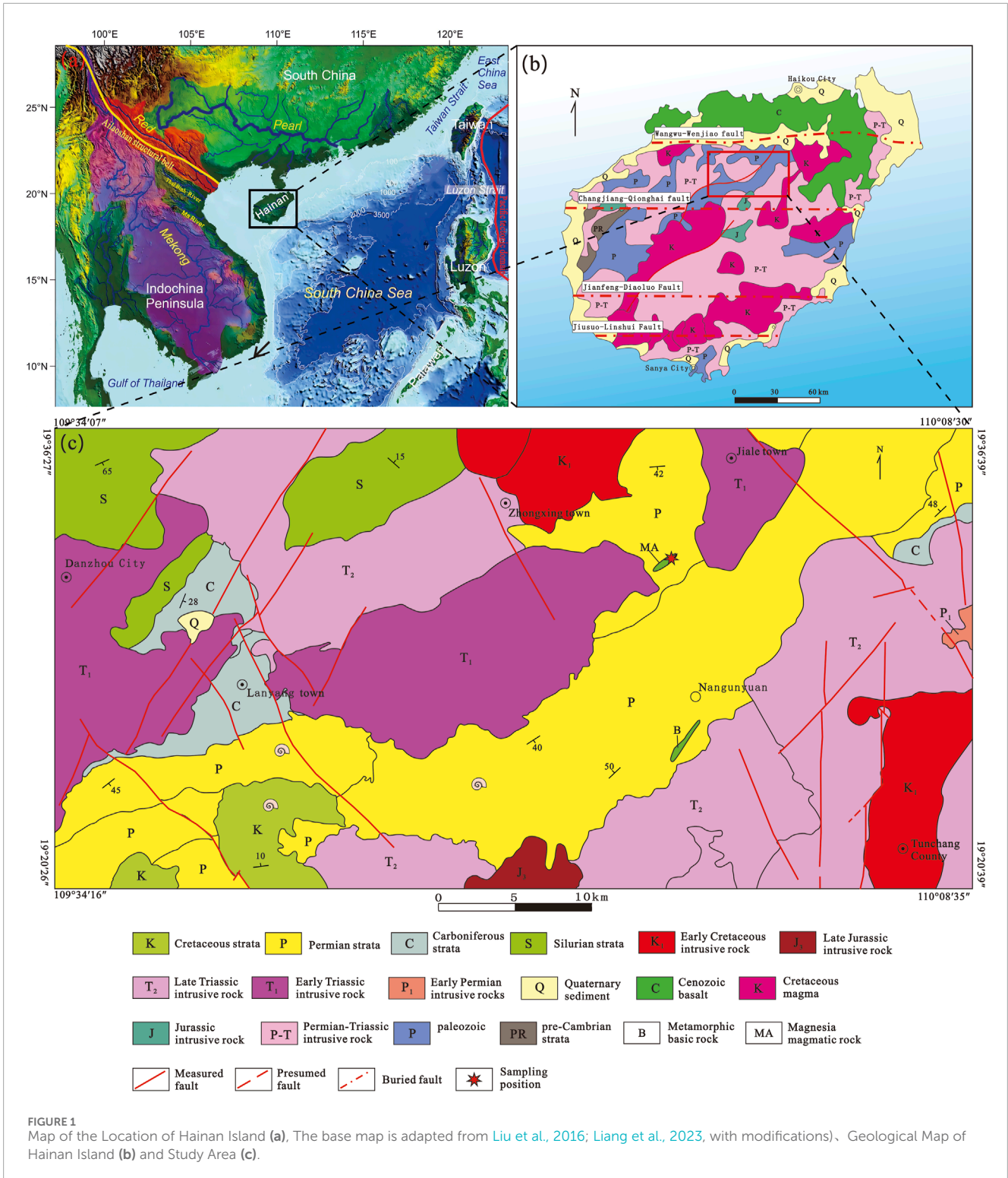
The stratigraphic record spans from Proterozoic to Cenozoic, excluding Devonian and Jurassic systems, with the Mesoproterozoic Baoban Group constituting the crystalline basement (Long et al., 2023). Intense magmatic activity is manifested through widespread Hercynian-Indosinian granitoids, predominantly biotite monzogranites and granodiorites, followed by Late Yanshanian intrusives (Wang et al., 2019). Volcanic sequences exhibit multi-phase eruptive histories, dominated by Cenozoic volcanics in northern Hainan, with subordinate Cretaceous continental intermediate-acid volcanic rocks in Mesozoic basins, while Proterozoic and Paleozoic volcanic units occur sporadically (Liang et al., 2021; Lin et al., 2022).

The Nangunyuan magnesian andesites in northern Hainan are located south of the Wangwu-Wenjiao Fault and north of the Changjiang-Qionghai Fault, specifically within the Nanchu Village area of Renxing Town, Chengmai County (Figure 1c). This region exposes several-kilometer-thick Paleozoic sedimentary sequences comprising flyschoid formations intercalated with volcanic and siliceous rocks, the latter containing radiolarian fossils indicative of pelagic environments (Long et al., 2007). Our field investigations identified newly discovered magnesian andesites occurring as interlayered and lenticular bodies within Late Paleozoic mudstones, argillaceous siltstones, silty mudstones, quartz sandstones, and siltstones (Figure 2a). These volcanic units strike NE-SW, concordant with regional bedding attitudes. The adjacent area hosts numerous Late Permian to Early-Middle Triassic monzogranite intrusions.

The magnesian andesites have undergone greenschist-facies metamorphism, with primary mineral assemblages largely replaced by secondary phases dominated by quartz (Figures 2b,c), actinolite (Figures 2b,c), zoisite, and epidote (Figure 2d). Rare relict clinopyroxene, diopside, and plagioclase crystals are locally preserved. Resultant metamorphic lithologies include quartz-actinolite schist, zoisite-actinolite rock, actinolite-diopside rock, quartz-epidote rock, quartz-plagioclase-epidote rock, and quartz-diopside rock, reflecting complex metasomatic overprinting during tectonic evolution.

Methods

The zircon separation was completed in the laboratory of the Hebei Regional Geological and Mineral Survey Research Institute. Conventional gravity and magnetic separation methods were used to separate zircon monominerals, and then zircons were handpicked under a binocular microscope. The zircons were placed on epoxy resin and then ground and polished to



expose the surface of the zircons. Cathodoluminescence (CL) microscopy was performed on the zircons to be dated. Zircon CL photography and LA-ICP-MS analysis were completed in the State Key Laboratory of Geological Processes and Mineral Resources at China University of Geosciences (Wuhan). CL photography was taken on a JEOL-JXA-8100 electron microprobe instrument. Zircon

U-Pb isotope and trace element content analyses were carried out using the GeoLas 2005 excimer laser ablation system from MicroLas Company on an Agilent7500a type ICP-MS instrument from Agilent Company in the United States. Zircon ages were calibrated externally using standard zircon 91,500, and GJ-1 was used as the internal standard sample. Element contents were calibrated

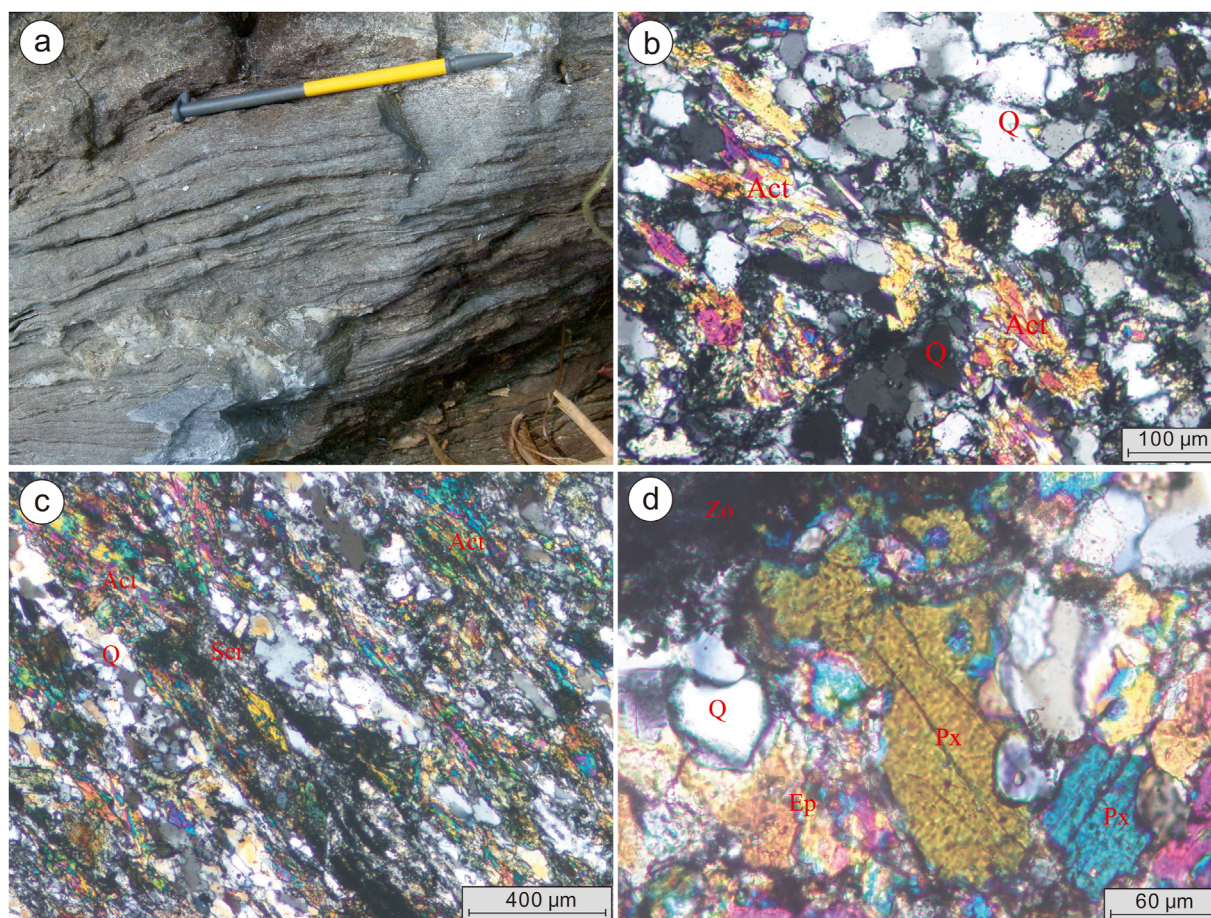


FIGURE 2

Field photograph (a) and photomicrograph (b–d) of magnesian andesitic samples of Northern Hainan Island Q: Quartz; Act: Actinolite; Ser: Sericite; Px: Pyroxene; Zo: Zoisite; Ep: Epidote.

externally using SRM610, with ^{29}Si as the internal standard element. ICP-MS-DataCal 8.3 was used for offline processing of the measured isotope data. The U-Pb age concordia diagram and weighted average age calculations and plots were completed using Isoplot 3.0. The error for individual data points is 1σ , and the confidence level for the weighted average age of the sample is 2σ , with a confidence level of 95%.

The analysis of whole-rock major elements, trace elements, and rare earth elements was completed in the Hubei Geological Experiment Research Institute. For major element analysis, except for H_2O , which was determined by gravimetric method, and CO_2 , which was analyzed by non-aqueous titration, the remaining oxides were determined by X-ray fluorescence spectroscopy with the a-coefficient method. The analytical precision (relative error) is 1% for all elements except H_2O . Trace elements and rare earth elements were analyzed using inductively coupled plasma atomic emission spectrometry (ICP-AES). The long-term (4 h) stability of this instrument is better than 1%, and the analytical precision is better than 1%. Spectral interferences were treated using a peak shaping function, i.e., Fitted background correction, to process the analyzed peak shapes.

Results

Zircon U-Pb age

The zircons in sample D0245-2 are mostly light rose or light brown in color, with a few being colorless and transparent. They are idiomorphic to subidiomorphic long columnar crystals, with lengths mostly ranging from 100 μm to 400 μm . The length-to-width ratios of the columnar crystals range from 2:1 to 4:1. CL images show distinct oscillatory zoning or platy zoning, which are typical characteristics of magmatic crystallization zircons (Figure 3). During LA-ICP-MS analysis, positions without inclusions and fractures were selected for measurement. Most of the selected positions are located at the edges of the zircons. The U and Pb test data of 20 points of zircons are shown in Table 1. The Th and U contents of the zircons range from 57 ppm to 1,695 ppm and 75 ppm–1970 ppm, respectively, with Th/U values between 0.25 and 1.04. The $^{206}\text{Pb}/^{238}\text{U}$ ages of the 20 measured points range from (244.5 ± 2.2) Ma to $(2,375.8 \pm 19.9)$ Ma. All the tested points are located on or near the concordia line. Among them, three points have $^{206}\text{Pb}/^{238}\text{U}$ ages greater than 1800 Ma, and two points have

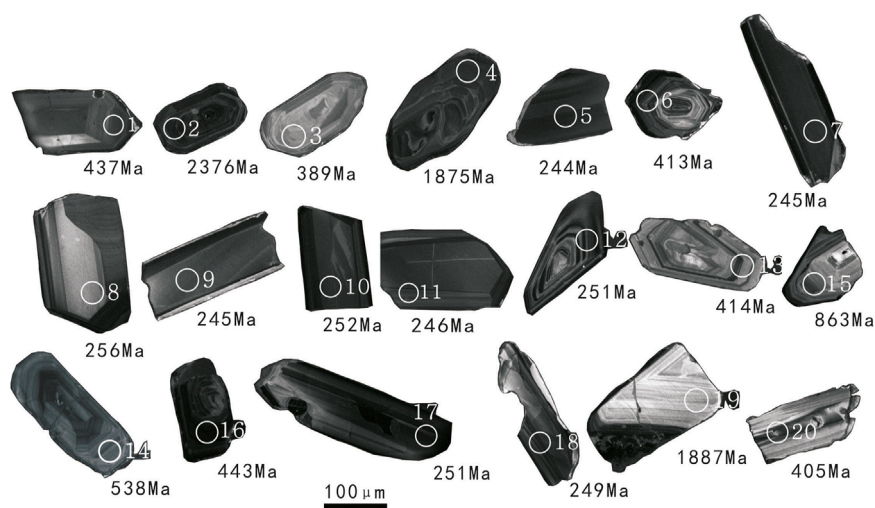


FIGURE 3
CL images of zircons from the magnesian andesitic samples.

$^{206}\text{Pb}/^{238}\text{U}$ ages of 862.6 ± 7.0 Ma and 537.8 ± 4.8 Ma, respectively. The remaining points are mainly distributed between 389–443 Ma and 244–256 Ma. Zircons at test points 7, 8, 9, 10, 11, and 17 exhibit broad platy zoning, which is a characteristic feature of zircons from typical neutral volcanic rocks. The weighted average $^{206}\text{Pb}/^{238}\text{U}$ age of these zircons is 251.2 ± 4.5 Ma (Figure 4). The obtained age of 251.2 ± 4.5 Ma can be interpreted as the eruption crystallization age of the volcanic rocks, while the other older $^{206}\text{Pb}/^{238}\text{U}$ ages may represent inherited zircon ages.

Major element

Due to the fact that the magnesian andesites in the Nangunyuuan area of northern Hainan Island occur as interlayers and lens-shaped bodies within Late Paleozoic metamorphic rocks, with small outcrop areas and strong rock weathering, only five fresh rock chemical samples were collected in this study. The chemical analysis results and main parameters of the rocks are listed in Table 2. The Al_2O_3 content of the magnesian andesite in the Nangunyuuan area of northern Hainan Island is relatively low. The aluminum saturation index A/CNK of most samples is less than 1, and the A/NK value is greater than 1, ranging from 1.93 to 3.22, indicating that they are metaluminous rocks. The Rittmann index σ ranges from 0.15 to 0.60, all less than 1. According to Rittmann's classification, they belong to the extremely strong Pacific-type within the alkali-calcic rock series. Based on the SiO_2 -Nb/Y diagram (Figure 5), they mainly fall into the rhyodacite/dacite series. Moreover, according to the Th-Co diagram (Figure 6), the samples all fall into the high-potassium calc-alkaline series and the olivine basalt series. The Magnesian-iron index (MF) value of the rocks is not large, ranging from 60.62 to 67.96, indicating that the degree of magmatic fractional crystallization is not high. The $\text{Mg}^\#$ value is moderate, ranging from 45.78 to 54.07, representing that the magma has undergone slight differentiation. The differentiation index (DI) is moderate, ranging from 41.15 to 59.70, close to the differentiation index (56) of the average chemical composition of Dacite, indicating that the degree of magmatic differentiation and

evolution is moderate. However, the solidification index (SI) value is relatively small, ranging from 25.61 to 28.17, indicating that the basicity of the rocks is moderate.

Rare earth element

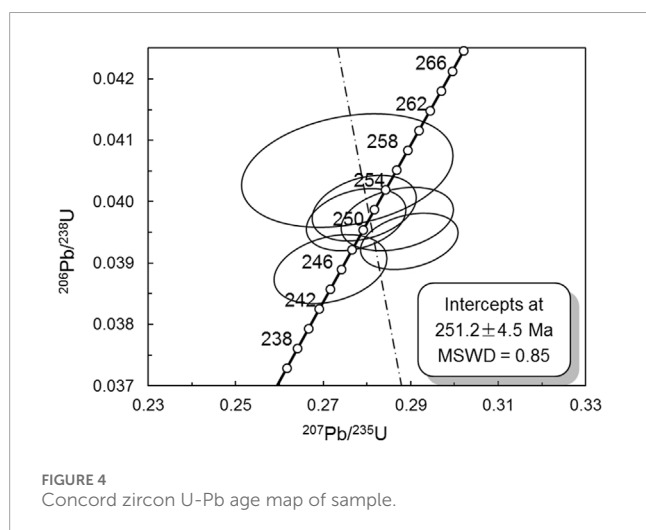
The total rare earth element (REE) contents of the five rocks do not vary significantly, and they generally exhibit similar REE distribution patterns (Figure 7), all showing right-leaning curves enriched in light rare earth elements (LREEs). The ratios of light to heavy rare earth elements range from 3.90 to 7.13; the $(\text{La}/\text{Yb})_N$ values range from 5.92 to 8.63, and the $(\text{Ce}/\text{Yb})_N$ values range from 1.71 to 5.12, indicating moderate differentiation between light and heavy rare earth elements. The $(\text{La}/\text{Sm})_N$ values range from 2.83 to 3.74 (with an average of 3.23), suggesting a slightly stronger fractionation among light rare earth elements. The $(\text{Gd}/\text{Yb})_N$ values range from 1.39 to 1.78, indicating that the fractionation among heavy rare earth elements is not significant, and the degree of fractionation of light rare earth elements is slightly stronger than that of heavy rare earth elements. The Eu element shows a moderate negative anomaly, with δEu values ranging from 0.67 to 0.74. The δCe values range from 0.29 to 0.90. Except for the D0245-1 sample, which has a δCe value of 0.9, showing a weak negative anomaly of the Ce element, the other samples exhibit a strong negative anomaly of the Ce element.

Trace element

The high field strength elements (HFS) Zr and Hf in the rocks have relatively high contents, while the contents of Nb and Ta are relatively low. The Nb/Ta ratios range from 8.4 to 13.46 (with an average of 11.5), all lower than those of chondrites, primitive mantle, mid-ocean ridge basalts ($\text{Nb}/\text{Ta} = 17.39$ – 17.66) (Anders and Grevesse, 1989; Sun and McDonough, 1989) and depleted mantle ($\text{Nb}/\text{Ta} = 14.29$) (McDonough, 1990), but close to that of the continental crust ($\text{Nb}/\text{Ta} = 11.43$) (Rudnick and Fountain, 1995). The large ion

TABLE 1 LA-ICP-MS zircon U-Pb results for the magnesian andesitic samples.

Point	Th	U	Th/U	²⁰⁷ Pb/ ²⁰⁶ Pb		²⁰⁷ Pb/ ²³⁵ U		²⁰⁶ Pb/ ²³⁸ U		²⁰⁷ Pb/ ²⁰⁶ Pb		²⁰⁷ Pb/ ²³⁵ U		²⁰⁶ Pb/ ²³⁸ U	
				Ratio	±1σ	Ratio	±1σ	Ratio	±1σ	Age	±1σ	Age	±1σ	Age	±1σ
1	857	1,036	0.83	0.0552	0.0012	0.5375	0.0118	0.0702	0.0005	420	54.6	437	7.8	437	3.0
2	364	634	0.57	0.1636	0.0028	10.1334	0.1908	0.4456	0.0045	2,494	28.7	2,447	17.5	2,376	19.9
3	211	212	1.00	0.0530	0.0024	0.4509	0.0194	0.0622	0.0007	328	106	378	13.6	389	4.0
4	189	504	0.38	0.1152	0.0022	5.3965	0.1066	0.3375	0.0026	1883	34.9	1884	17.0	1875	12.5
5	730	996	0.73	0.0493	0.0015	0.2625	0.0080	0.0387	0.0004	167	74.1	237	6.5	244	2.2
6	242	707	0.34	0.0548	0.0016	0.5019	0.0143	0.0662	0.0006	467	69.4	413	9.7	413	3.5
7	1,695	1,637	1.04	0.0506	0.0012	0.2719	0.0065	0.0387	0.0003	233	55.5	244	5.2	245	1.9
8	62	238	0.26	0.0505	0.0031	0.2755	0.0160	0.0405	0.0006	220	144	247	12.7	256	3.8
9	199	561	0.35	0.0506	0.0018	0.2713	0.0095	0.0390	0.0004	233	52.8	244	7.6	246	2.6
10	624	932	0.67	0.0504	0.0014	0.2794	0.0079	0.0399	0.0004	213	66.7	250	6.2	252	2.2
11	542	903	0.60	0.0504	0.0016	0.2717	0.0085	0.0389	0.0004	213	41.7	244	6.8	246	2.3
12	276	1,129	0.24	0.0504	0.0014	0.2775	0.0075	0.0397	0.0003	213	63.0	249	6.0	251	2.1
13	162	340	0.48	0.0551	0.0019	0.5063	0.0174	0.0664	0.0007	413	74.1	416	11.7	414	4.4
14	131	354	0.37	0.0587	0.0018	0.7047	0.0215	0.0870	0.0008	554	75.0	542	12.8	538	4.8
15	64	238	0.27	0.0724	0.0020	1.4359	0.0401	0.1432	0.0012	998	57.4	904	16.7	863	7.0
16	784	1970	0.40	0.0579	0.0013	0.5718	0.0130	0.0712	0.0006	524	48.1	459	8.4	443	3.4
17	645	739	0.87	0.0523	0.0016	0.2869	0.0085	0.0397	0.0003	302	70.4	256	6.7	251	2.1
18	1,097	1,216	0.90	0.0531	0.0013	0.2897	0.0074	0.0394	0.0003	345	57.4	258	5.8	249	1.9
19	57	75	0.75	0.1176	0.0030	5.5320	0.1407	0.3401	0.0032	1921	44.6	1906	21.9	1887	15.5
20	240	277	0.86	0.0602	0.0022	0.5382	0.0198	0.0648	0.0007	613	78.5	437	13.1	405	4.0



lithophile elements are significantly enriched. On the trace element spider diagram (Figure 8), the trace element spider distribution curves of the five rock samples are basically consistent. They are characterized by the strong incompatible elements such as Rb, Ba, Th, K being more enriched than the moderately incompatible elements such as Sr, Nb, P, Zr. Among them, Rb, Th, U, K, La, Pb, Pr, Nd, Sm, Gd show significant positive anomalies on the trace element ratio spider diagram, while Cs, Ba, Nb, Ce, P, Zr, Ti show obvious negative anomalies.

Discussion

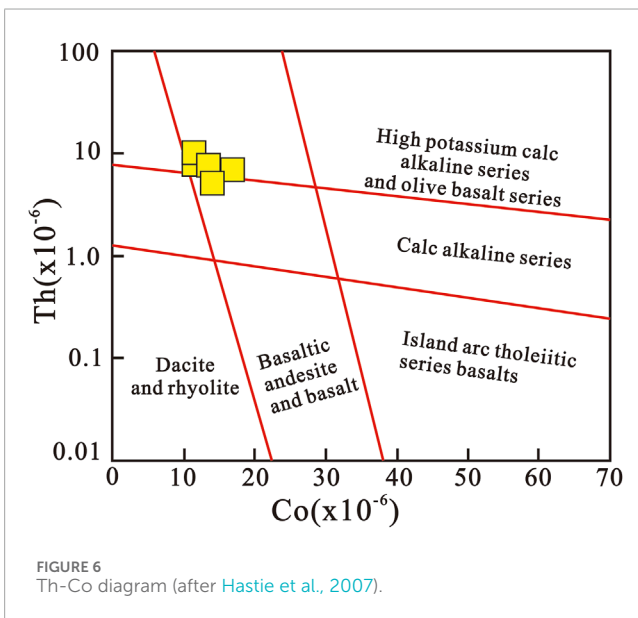
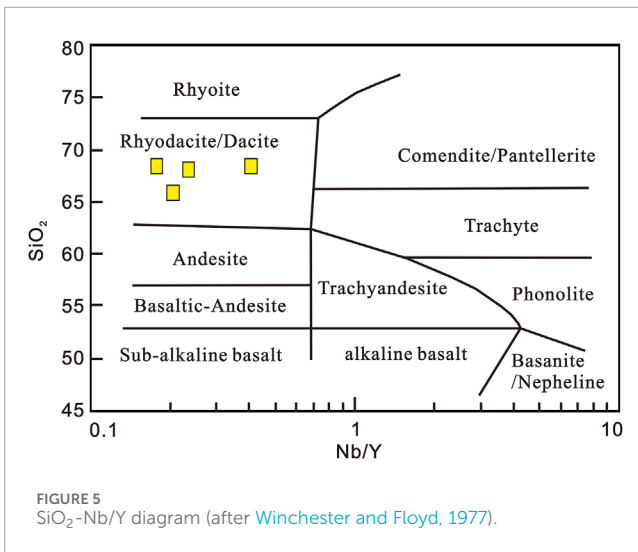
Petrogenesis of magnesian andesite

Current petrogenetic models for magnesian andesites primarily include: (1) assimilation-fractional crystallization (AFC) of mantle-derived basaltic magmas (Macpherson et al., 2006);

TABLE 2 Chemical composition of main (wt%) and trace elements ($\times 10^{-6}$) of magnesia Andesitic rocks in Nanchuyuan area, Northern Hainan Island.

Sample number	SiO ₂	TiO ₂	Al ₂ O ₃	Fe ₂ O ₃	FeO	MnO	MgO	CaO	Na ₂ O	K ₂ O	P ₂ O ₅	CO ₂	FeO ^T	FeO ^T /MgC	Mg [#]	A/CNK	A/NK	MF
TC036-2-1	68.44	0.59	10.01	0.81	4.30	0.06	3.32	7.71	1.89	1.47	0.14	0.06	5.03	1.52	54.07	0.54	2.13	60.62
TC036-8-1	65.89	0.59	10.46	0.38	5.25	0.11	2.97	10.34	1.77	1.12	0.12	0.12	5.59	1.88	48.64	0.46	2.54	65.47
T036-8-2	62.60	0.49	8.96	0.34	7.00	0.17	3.46	13.89	1.58	0.17	0.11	0.19	7.31	2.11	45.78	0.32	3.22	67.96
D0245-2	68.12	0.55	10.21	0.79	4.13	0.24	3.03	7.68	1.93	1.95	0.14	0.22	4.84	1.60	52.74	0.53	1.93	61.89
D0245-1	68.43	0.67	10.87	0.18	5.00	0.06	3.22	7.13	1.25	1.78	0.13	0.12	5.16	1.60	52.65	0.64	2.73	61.67
σ		La	Ce	Pr	Nd	Sm	Eu	Gd	Tb	Dy	Ho	Er	Tm	Yb	Lu	Y	L/H	δ Eu
TC036-2-1	0.44	69.49	44.17	18.45	71.28	14.4	3.23	12.01	2.12	10.61	1.94	5.20	0.80	5.43	0.76	46.23	5.68	0.73
TC036-8-1	0.36	43.24	50.56	10.35	41.00	8.44	2.05	8.35	1.53	8.15	1.64	4.41	0.65	4.13	0.60	46.44	5.28	0.74
T036-8-2	0.15	55.84	42.16	14.00	56.16	12.4	3.11	12.93	2.48	13.44	2.71	7.21	1.01	6.36	0.90	79.23	3.90	0.74
D0245-2	0.60	39.90	51.30	8.67	31.60	6.71	1.55	6.45	1.07	5.95	1.19	3.06	0.48	3.20	0.50	32.20	6.38	0.71
D0245-1	0.36	28.00	53.21	6.82	26.27	5.33	1.12	4.64	0.80	4.65	0.87	2.51	0.39	2.69	0.38	23.67	7.13	0.67
δ Ce		(Dy/Yb) _N	(La/Yb) _N	(Ce/Yb) _N	(La/Sm) _N	(Gd/Yb) _N	Y/Yb	Sr/Y	Rb	Sr	Ba	Zr	Ta	Hf	Nb	Ni	Th	Co
TC036-2-1	0.29	1.31	8.63	2.10	3.05	1.78	8.51	4.29	63.44	198.10	414.3	141.80	0.61	4.38	8.21	33.67	7.53	17.10
TC036-8-1	0.56	1.32	7.06	3.17	3.22	1.63	11.24	4.94	50.08	229.60	237.7	131.10	1.00	4.20	9.53	22.31	7.61	13.60
T036-8-2	0.35	1.41	5.92	1.71	2.83	1.64	12.46	2.75	9.33	217.80	101.5	108.30	0.42	3.83	5.40	16.28	5.53	14.00
D0245-2	0.64	1.24	8.41	4.15	3.74	1.63	10.06	5.59	81.80	180.00	323.00	131.00	0.57	4.08	7.55	35.6	8.80	120.00
D0245-1	0.90	1.16	7.02	5.12	3.30	1.39	8.80	7.85	63.68	185.8	256.50	159.8	1.14	5.34	9.58	29.27	9.66	11.50
U		V	Cr	Cu	Zn	Pb	Ga	Li	Cs	Zr/Nb	Ba/Nb	Ba/Th	Rb/Nb	Th/Nb	Th/La	Zr/Hf	Nb/Ta	
TC036-2-1	1.80	112.00	54.63	17.60	106.20	14.38	12.56	6.94	2.11	17.27	55.02	55.02	7.73	0.92	0.11	32.40	13.46	
TC036-8-1	1.80	110.00	53.29	13.30	113.70	15.08	14.24	12.24	2.95	13.76	24.94	31.24	5.27	0.80	0.18	31.20	9.53	
T036-8-2	1.37	93.00	45.11	2.93	141.20	8.21	12.31	15.35	2.13	20.06	18.80	18.35	1.73	1.02	0.10	28.30	12.86	
D0245-2	2.02	96.90	41.60	59.30	98.80	17.80	13.10	28.30	2.39	17.35	42.78	26.70	10.83	1.17	0.22	32.10	13.25	
D0245-1	2.26	117.00	57.29	36.40	100.30	20.18	15.00	8.25	2.94	16.68	26.77	26.55	6.65	1.01	0.35	29.90	8.40	

note: Mg[#] = 100xMg/(Mg + Fe²⁺), L/H = LREE/HREE.



(2) partial melting of hydrous mantle peridotite (Straub et al., 2011); (3) reaction between delaminated lower crust and mantle peridotite (Xu et al., 2002); (4) mixing of crustal felsic and mantle-derived basaltic magmas (Streck et al., 2007); and (5) metasomatic interactions between subducted slab melts/sediment melts/slab-derived fluids and overlying mantle wedge (Dong and Santosh, 2016).

The Nangunyan magnesian andesites in northern Hainan Island exhibit elevated SiO₂ (53.12–58.34 wt%), CaO (6.23–8.15 wt%), and MgO (5.67–7.89 wt%) contents, coupled with relatively low Na₂O (2.12–3.45 wt%), K₂O (0.78–1.56 wt%), and Fe₂O₃ (6.34–7.89 wt%) concentrations. Their position within the LF-CA field on the SiO₂-FeO*/MgO diagram (Figure 9) confirms their classification as magnesian andesites, precluding their origin from partial melting of basaltic rocks. Delamination models typically operate under crustal thickening conditions with garnet as the dominant residual phase. Given the strong

compatibility of heavy rare earth elements (HREEs) and Y in garnet, significant HREE and Y depletion serves as a diagnostic indicator of garnet residue (Xu et al., 2002). However, the studied samples display low (Dy/Yb)_N ratios (1.16–1.41), coupled with elevated Yb (2.69–6.36 ppm) and Y (23.67–79.23 ppm) concentrations, demonstrating the absence of substantial garnet residues in their source. Furthermore, delaminated lower crust melting typically generates high Sr/Y adakites with Mg[#] <45 (Huang et al., 2007), whereas the Mg[#] values of these andesites range from 45.78 to 54.07, systematically exceeding the threshold. These geochemical contradictions effectively exclude the delamination-peridotite reaction model as a viable mechanism for the Nangunyan magnesian andesites.

The magnesian andesites from the Nangunyan area in northern Hainan Island exhibit diagnostic arc volcanic signatures, as evidenced by their elevated Zr/Nb ratios (13.76–20.06), low Nb/La (0.091–0.342), and Nb/Th ratios (0.858–1.252) – geochemical parameters characteristic of typical island arc systems. These rocks display marked enrichment in large-ion lithophile elements (LILEs) coupled with relative depletion of high-field-strength elements (HFSEs), accompanied by pronounced negative anomalies in Ta, Nb, and Ti, features consistent with active continental margin or arc volcanic settings. The HFSEs (Zr, Hf, Nb, Ta), being relatively immobile during alteration and metamorphic processes, serve as robust tracers for source characterization. Ratios between these elements (Nb/Ta, Zr/Nb) provide critical petrogenetic constraints, particularly given the limited fractionation of Nb/Ta ratios during mantle partial melting or magmatic differentiation. The studied andesites show Nb/Ta ratios (average 11.5) comparable to continental crust values (11–13), while their Zr/Nb ratios align with primitive mantle compositions. This dual signature implies significant crustal contamination during magma evolution. Further confirmation comes from immobile element discrimination diagrams: The Nb/Th versus Nb plot (Figure 10) and Ce/Pb versus Ce systematics (Figure 11) consistently classify these rocks within the arc volcanic field. The integrated geochemical evidence demonstrates that crustal material incorporation played a pivotal role in modifying mantle-derived magmas, likely through subduction-related processes involving slab-derived fluids or sediment melts.

The Sanukite from the Setouchi region of Japan represents a typical island arc volcanic rock, characterized by high silica content and elevated Mg, Cr, and Ni concentrations (Tatsumi, 2008). Although the magnesian andesites from Nangunyan area in northern Hainan Island plot within the sanukite field on the Y-Sr/Y diagram (Figure 12) and share similar geochemical signatures with sanukite, they exhibit notably lower MgO (Mg[#]), Ni, and Cr contents compared to the Japanese Sanukite. The Nb/Ta ratios of these Hainan samples range from 8.4 to 13.46 (average 11.5), consistently lower than those of chondrites (17.5), primitive mantle (17.5), mid-ocean ridge basalts (15–16), and depleted mantle, but comparable to continental crust values (11–13). In the Zr-(Nb/Zr)_N classification diagram (Figure 13), the Hainan magnesian andesites predominantly fall within the subduction-related rock field.

The Th/Nb-Ce/Nb systematics (Figure 14) further indicate that these rocks plot near arc volcanic magma fields, suggesting

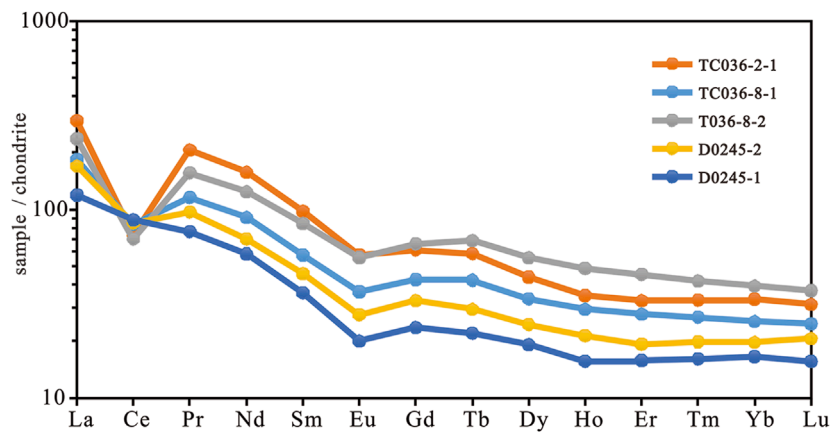


FIGURE 7 Chondrite-normalized REE patterns (normalized data after Anders and Grevesse, 1989).

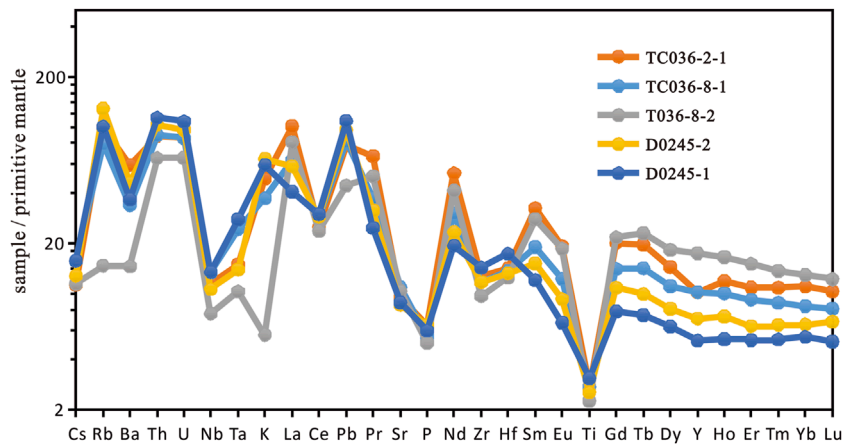


FIGURE 8 Primitive mantle-normalized trace element patterns (normalized data after Anders and Grevesse, 1989).

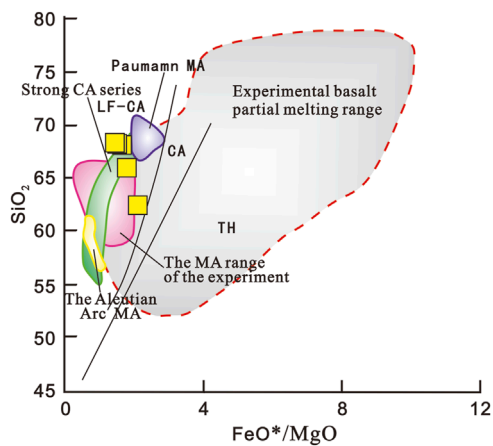


FIGURE 9 SiO_2 - FeO^*/MgO diagram MA: Magnesian Andesite; CA: Calc-Alkaline; LF-CA: Low Fe Calc-alkaline; TH: Tholeiite.

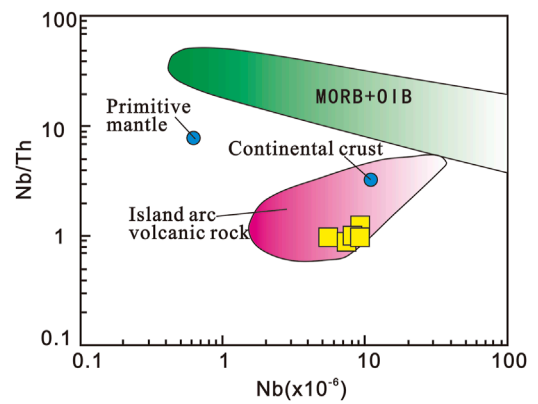
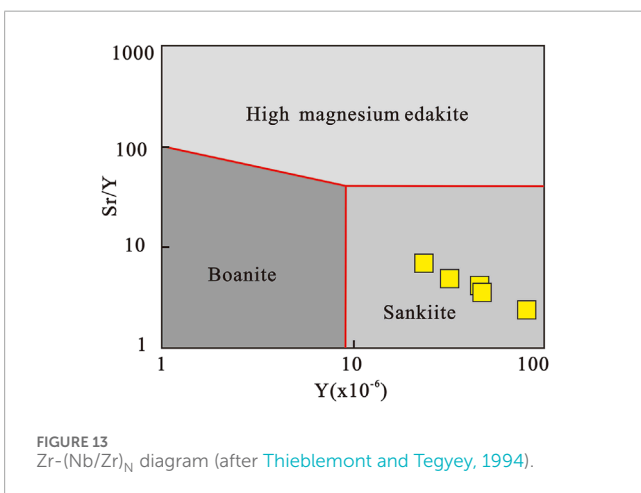
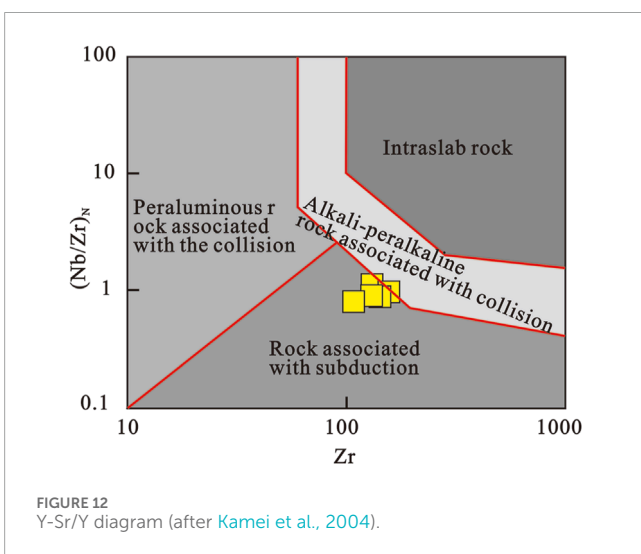
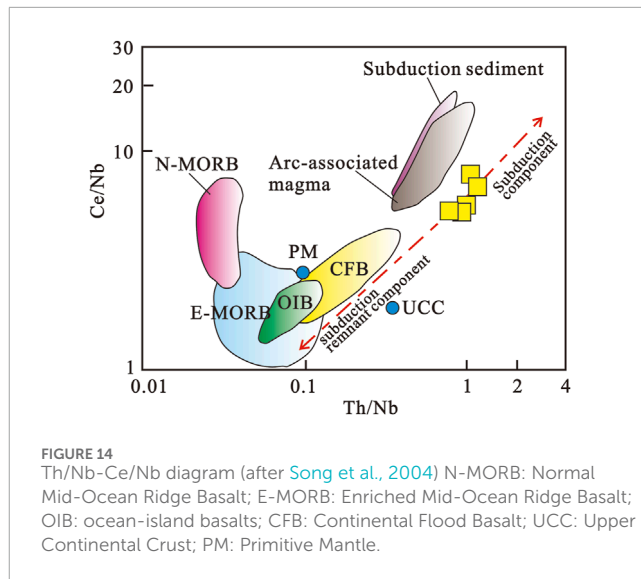
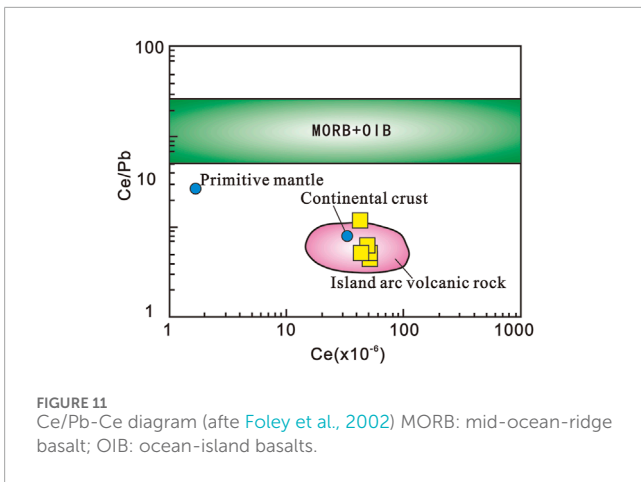


FIGURE 10 Nb/Th-Nb diagram (after Li et al., 2015) MORB: mid-ocean-ridge basalt; OIB: ocean-island basalts.



their magmatic formation might be associated with arc-related processes. This implies potential incorporation of deep-sea sediments or crustal materials into their source region. Petrogenetic modeling supports a source region formed through metasomatic reactions between mantle peridotite and Si-rich

melts derived from partial melting of subducted oceanic crust or sediments (Figure 15). In contrast, the Setouchi sanukite originates from mantle wedge environments in subduction zones, representing typical products of crust-mantle interaction (Tatsumi, 2008).

While the Hainan magnesian andesites share genetic similarities with typical arc-related rocks from Setouchi in terms of geochemical characteristics and formation mechanisms, their distinct compositional differences reflect unique tectonic-magmatic evolutionary processes in different regional settings. Comparatively, these Hainan rocks exhibit analogous petrogenetic patterns to magnesian andesites from the northeastern margin of the North China Craton (Guo et al., 2022) and the Qinling orogen (Li et al., 2020), all originating from hybrid sources involving interactions between subducted slab-derived melts (or sediments) and mantle peridotite.

Geotectonic significance

The EW-trending Changjiang-Qionghai Fault in Hainan Island was initially inferred from contrasting geological and geophysical characteristics across its northern and southern sectors. However, its tectonic nature and final amalgamation age remain contentious. Along the fault's northern flank (Junying, Bangxi, Bayi Farm, Nanfeng, Chenxing Farm, Zhongrui Farm), discontinuous meta-volcanic rocks ranging from acidic to ultramafic compositions have been identified, predominantly mafic lithologies occurring as stratiform, lenticular, or irregular bodies within Paleozoic deep-to shallow-marine metasedimentary sequences. Over the past 2 decades, multidisciplinary studies have proposed three principal genetic models: 1. Late Paleozoic bimodal volcanic suites representing intracontinental rifting (Xia and Shi, 1991) or coeval Paleo-Tethyan oceanic basin development (Tang, 1999); 2. Mesoproterozoic komatiitic basalts indicative of Paleoproterozoic subduction and Meso-Neoproterozoic crustal breakup (Zhang et al., 1998; Liang et al., 2000; Xu et al., 2001); 3. Mid-ocean ridge basalt (MORB) or ocean island basalt (OIB) assemblages interpreted as

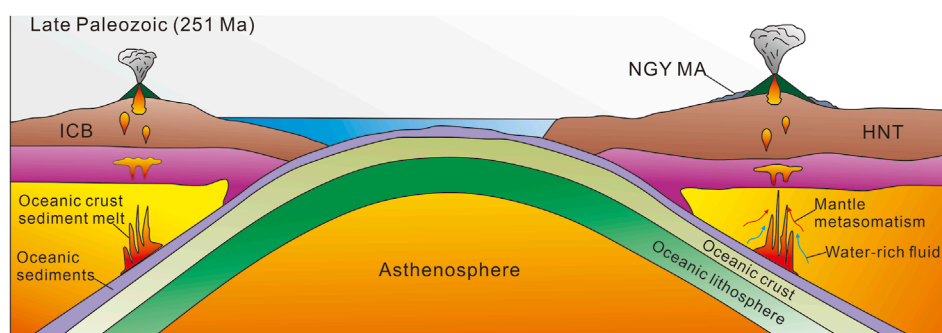


FIGURE 15

Genesis and tectonic model diagram of Magnesium andesite ICB: Indochina Block; HNT: Hainan terrane; NGY MA: Nangunyan magnesian andesite.

remnants of the eastern Paleo-Tethyan oceanic crust (Li et al., 2000b) or coeval Paleo-Tethyan basins (Wang et al., 2013; Metcalfe, 2021). These conflicting interpretations, largely based on localized lithological observations, fail to reconcile regional tectonic coherence. Xu et al. (2006) proposed a temporal-spatial framework: Mafic lavas at Chenxing Farm (Tunchang County) may record ~450 Ma Early Paleozoic oceanic crust, while Junying-Bangxi mafic rocks potentially reflect ~270 Ma back-arc spreading during Late Paleozoic subduction of the eastern Paleo-Tethyan Ocean beneath the South China margin. Peak subduction of the eastern Paleo-Tethyan Ocean occurred during the Carboniferous-Permian, with its closure constrained to ~237–247 Ma (Xu et al., 2019; Yu et al., 2022). The Nangunyan magnesian andesites in northern Hainan, dated to this interval, likely represent terminal-stage subduction processes. Supporting evidence includes N-MORB-type amphibolite-facies metabasites along the Changjiang-Qionghai Fault (Li et al., 2000a), geochemically correlative with the Jinshajiang-Song Ma ophiolites, suggesting Hainan's Late Paleozoic basin constituted the easternmost Paleo-Tethyan extension. Petrogenetic models posit that hydrous slab-derived fluids metasomatized the mantle wedge, generating Mg-rich melts that mixed with peridotite to form magnesian andesites—a process confirming active Paleo-Tethyan subduction persisting into the Late Permian (Figure 15).

Conclusion

The Mg andesite in the Nangunyan area of northern Hainan Island occurs as interbeds and lenses in late Paleozoic strata. It belongs to the neutral to acidic rock association of the high-potassium calc-alkaline series - olivine basalt series. The rocks are characterized by relatively high contents of SiO₂, CaO, and MgO, and relatively low contents of Na₂O, K₂O, and Fe₂O₃. Moreover, the Mg[#] values range from 45.78 to 54.07. The petrogeochemical characteristics of the rocks indicate features of magnesian andesite. Geochemical discrimination diagrams suggest that the rocks possess typical island-arc volcanic features and belong to island-arc volcanic rocks.

These rocks exhibit geochemical affinities comparable to sanukite-type magmas, yet display distinctively lower MgO, Ni, and Cr concentrations relative to typical sanukites. Their Nb/Ta ratios (8.4–13.46) align with continental crustal values, suggesting source contamination through incorporation of deep-sea sediments or crustal materials. Petrogenetic modeling supports formation via metasomatic reactions between mantle peridotite and Si-rich melts derived from partial melting of subducted oceanic slabs/sediments. This geochemical fingerprint implies the operation of arc-active continental margin subduction systems during the Late Paleozoic. In future research, Sr-Nd-Hf isotope analysis and zircon U-Pb isotopic dating will be supplemented to enhance the argumentation basis and render the results more reliable.

(3) LA-ICP-MS zircon U-Pb dating constrains the magnesian andesites' emplacement age to 251.2 ± 4.5 Ma (Late Permian), temporally coincident with the terminal closure of the eastern Paleo-Tethys Ocean (~237–247 Ma). This chronological correlation positions their formation within the waning stages of Paleo-Tethyan subduction. Our findings provide critical constraints for refining the closure timeline of the eastern Paleo-Tethyan Ocean, deciphering the geodynamic mechanisms of Paleo-Tethyan orogenesis and elucidating metallogenic processes in convergent margin settings, thereby enhancing our understanding of East Asian tectonic evolution.

Data availability statement

The original contributions presented in the study are included in the article/supplementary material, further inquiries can be directed to the corresponding authors.

Author contributions

YL: Conceptualization, Funding acquisition, Investigation, Project administration, Resources, Writing – original draft, Writing – review and editing. DL: Formal Analysis, Investigation,

Methodology, Project administration, Software, Writing – original draft, Writing – review and editing. ZH: Investigation, Validation, Writing – original draft, Writing – review and editing. QY: Investigation, Writing – review and editing. ZL: Investigation, Methodology, Validation, Writing – review and editing. JG: Data curation, Investigation, Writing – review and editing.

Funding

The author(s) declare that financial support was received for the research and/or publication of this article. This work was funded by The Key Laboratory of Marine Geological Resources and Environment of Hainan Province Project (No. HNHYZZZYHJZZ002), the project of geological survey of China (No. 1212011220524) and the Hainan Provincial Natural Science Foundation of China (No. 420RC744).

References

- Anders, E., and Grevesse, N. (1989). Abundances of the elements: meteoritic and solar. *Geochim. Cosmochim. Acta*. 53, 197–214. doi:10.1016/0016-7037(89)90286-x
- Ashraf, U., Zhang, H., Anees, A., Zhang, X., and Duan, L. (2024). Assessment of lake-level variations to decipher geological controlling factors and depositional architecture of Lake Fuxian, Yunnan Plateau: preliminary insights from geophysical data. *Geomechanics Geophys. Geo-Energy Geo-Resources* 10 (1), 64. doi:10.1007/s40948-024-00777-7
- Chao, H., Han, X., Yang, Z., Wu, X., Lv, Y., Yang, H., et al. (2016). New exploration of geotectonic characteristics of Hainan Island. *Earth Sci. Front.* 23, 200–211. doi:10.13745/j.esf.2016.04.017 (in Chinese with English abstract).
- Deng, F., Liu, C., Feng, Y., Xiao, Q., Su, S., Zhao, G., et al. (2010). High magnesian andesitic/dioritic rocks(HMA) and magnesian andesitic/dioritic rocks(MA):two igneous rock types related to oceanic subduction. *Geol. China* 37, 1112–1118. (in Chinese with English abstract).
- Ding, S., Hu, J., Song, B., Chen, M., Xie, S., and Fan, Y. (2005). Zircon U–Pb dating of bedding emplacement deep fused granites and its tectonic implications in Baoban Group, Hainan Island. *Sci. Sin.* 35, 33–44. (in Chinese with English abstract).
- Dong, Y., and Santosh, M. (2016). Tectonic architecture and multiple orogeny of the Qinling orogenic belt, Central China. *Gondwana Res.* 29, 1–40. doi:10.1016/j.gr.2015.06.009
- Foley, S., Tiepolo, M., and Vannucci, R. (2002). Growth of early continental crust controlled by melting of amphibolite in subduction zones. *Nature* 417, 837–840. doi:10.1038/nature00799
- Gao, Y., Li, X., Gu, P., Ma, Z., Zhuang, Y., Guo, Z., et al. (2022). The geodynamic setting of Triassic large-scale mineralization event in the West Qinling Orogen: evidence from high-Mg andesite in the Qiadong copper deposit. *Acta Petrol. Sin.* 38, 3143–3164. doi:10.18654/1000-0569/2022.10.15
- Gou, Q., Qian, X., He, H., Zhang, Y., and Wang, Y. (2019). Geochronological and geochemical constraints on lizhigou middle triassic felsic volcanic rocks in hainan and its tectonic implication. *Earth Sci.* 44, 1357–1370. (in Chinese with English abstract).
- Guo, R., Li, Z., and Huang, X. (2022). Petrogenesis for late neoproterozoic high magnesian andesites in the anshan-benxi Area, *Journal of Northeastern University (Natural Science)*, 43, 740–747. doi:10.12068/j.issn.1005-3026.2022.05.019 (in Chinese with English abstract).
- Hastie, A., Kerr, A., Pearce, J., and Mitchell, S. (2007). Classification of altered volcanic island arc rocks using immobile trace elements: development of the Th–Co discrimination diagram. *J. Petrology* 48, 2341–2357. doi:10.1093/petrology/egm062
- He, H., Wang, Y., Zhang, Y., Chen, X., and Zhou, Y. (2016). Extremely depleted carboniferous N-MORB metabasite at the chenxing area (hainan) and its geological significance. *Earth Sci.* 41, 1361–1375. (in Chinese with English abstract).
- Huang, H., Gao, S., Hu, Z., Liu, X., and Yuan, H. (2007). Geochemistry of Mesozoic high-Magnesian andesites in the Changwu area, western Liaoning Province, and their indications for deconstruction and subsidence of the Cenozoic lower crust. *Sci. China Series D: Earth Sci.* 10, 1287–1300. (in Chinese with English abstract).
- Kamei, A., Owada, M., Nagao, T., and Shiraki, K. (2004). High-Mg diorites derived from sanukitic HMA magmas, Kyushu Island, southwest Japan arc: evidence from clinopyroxene and whole rock compositions. *Lithos* 75, 359–371. doi:10.1016/j.lithos.2004.03.006
- Li, K., Liu, B., and Di, Y. (2020). Triassic oceanic subduction in northwestern west Qinling mountain: evidence from MA/HMA. *Geol. China*. 47, 709–724. (in Chinese with English abstract).
- Li, X., Zhou, H., Chung, S., Ding, S., Liu, Y., Lee, C., et al. (2002). Geochemical and Sm–Nd isotopic characteristics of metabasites from Central Hainan Island, South China and their tectonic significance. *Isl. Arc* 11, 193–205. doi:10.1046/j.1440-1738.2002.00365.x
- Li, X., Zhou, H., Ding, S., Li, J., Zhang, R., Zhang, Y., et al. (2000a). Mid-ocean ridge metamorphic mafic rocks of hainan island: fragments of the paleo-tethys oceanic crust? *Chin. Sci. Bull.* 45, 84–89. (in Chinese with English abstract).
- Li, X., Zhou, H., Ding, S., Li, J., Zhang, R., Zhang, Y., et al. (2000b). Sm–Nd isotopic constraints on the age of the Bangxi–Chenxing ophiolite in Hainan Island: implications for the tectonic evolution of eastern Paleo-Tethys. *Acta Petrol. Sin.* 16, 425–432. (in Chinese with English abstract).
- Li, Y., Li, G., Tong, L., Yang, G., and Wang, R. (2015). Discrimination of ratios of Ta, Hf, Th, La, Zr and Nb for tectonic settings in basalts. *J. Earth Sci. Environ.* 37, 14–21. (in Chinese with English abstract).
- Liang, D., Li, S., Wei, C., Wang, Y., Zhou, J., Lin, Y., et al. (2018). Geochemical characteristics and its paleoclimatic implications of holocene beach rocks in the southwest hainan island. *J. Stratigr.* 42, 108–116. (in Chinese with English abstract).
- Liang, D., Xu, G., Gao, F., Wen, L., Jia, L., Liu, L., et al. (2023). Holocene sediment source analysis and paleoclimatic significance of core KZK01 from the eastern part of the Beibu Gulf. *Front. Earth Sci.* 11, 1192206. doi:10.3389/feart.2023.1192206
- Liang, D., Xu, G., Xiao, Y., Chen, X., Li, S., Ruan, M., et al. (2021). Neogene-quaternary stratigraphic standard and combined zoning of haikou jiangdong new district. *Sci. Technol. Eng.* 21, 11052–11063. (in Chinese with English abstract).
- Liang, X., Fan, W., and Xu, D. (2000). Sm–Nd age of tunchang basaltic komatiites and its geological significance in hainan island. *Chin. J. Geol.* 35, 240–244. (in Chinese with English abstract).
- Lin, Y., Lv, Z., Yuan, Q., Wang, C., and Hu, Z. (2022). Determination of the early cretaceous volcanic stratum in wuzhishan area, Hainan island. *Mineral Resour. Geol.* 36, 796–804. (in Chinese with English abstract).
- Liu, F., Yang, J., Feng, G., Niu, X., Li, G., and Zhang, C. (2022a). Late permian to early triassic subduction and retreating of the paleopacific slab: constraints from continental arc magmatism in hainan island. *Acta Petrol. Sin.* 38, 3455–3483. doi:10.18654/1000-0569/2022.11.12

Conflict of interest

The authors declare that the research was conducted in the absence of any commercial or financial relationships that could be construed as a potential conflict of interest.

Generative AI statement

The author(s) declare that no Generative AI was used in the creation of this manuscript.

Publisher's note

All claims expressed in this article are solely those of the authors and do not necessarily represent those of their affiliated organizations, or those of the publisher, the editors and the reviewers. Any product that may be evaluated in this article, or claim that may be made by its manufacturer, is not guaranteed or endorsed by the publisher.

- Liu, X., Hu, J., Xia, M., Han, J., and Hu, D. (2022b). The Mulantou metamorphic from northeastern Hainan Island, South China: compositions, ages and tectonic implications. *Acta Geol. Sin.* 96, 3051–3083. (in Chinese with English abstract).
- Liu, X. C., Chen, Y., Wang, W., Xia, M., Hu, J., Li, Y., et al. (2021). Carboniferous eclogite and garnet-omphacite granulite from northeastern Hainan Island, South China: Implications for the evolution of the eastern Palaeo-Tethys. *J. Metamorph.* 39, 101–132. doi:10.1111/jmg.12563
- Liu, Z. F., Zhao, Y. L., Colin, C., Statterger, K., Wiesner, M. G., Huh, C. A., et al. (2016). Source-to-sink transport processes of fluvial sediments in the South China Sea. *Earth-Sci Rev.* 153, 238–273. doi:10.1016/j.earscirev.2015.08.005
- Long, W., Tong, J., Zhu, Y., Zhou, J., Li, S., and Shi, C. (2007). Discovery of the permian in the danzhou-tunchang area of hainan island and its geological significanc. *South China Geol.* 8, 38–45. (in Chinese with English abstract).
- Long, W., Wang, J., Wu, J., Zhang, J., Zhou, D., and Wang, X. (2023). Re-Disintegration of the Former “Baoban Group” in the huangzhuling area, eastern hainan island. *J. Stratigr.* 47, 80–90. (in Chinese with English abstract).
- Lv, F., Xin, Y., Li, J., and Wang, J. (2023). Permian-Triassic tectonic evolution of Hainan Island geochronology and geochemistry of magmatic and metamorphic rocks. *Acta Geol. Sin.* 97, 30–51. (in Chinese with English abstract).
- Macpherson, C., Dreher, S., and Thirlwall, M. (2006). Adakites without slab melting: high pressure differentiation of island arc magma, Mindanao, the Philippines. *Earth Planet. Sci. Lett.* 243, 581–593. doi:10.1016/j.epsl.2005.12.034
- McDonough, W. (1990). Constraints on the composition of the continental lithospheric mantle. *Earth Planet. Sci. Lett.* 101, 1–18. doi:10.1016/0012-821x(90)90119-i
- Metcalfe, I. (2021). Multiple Tethyan ocean basins and orogenic belts in Asia. *Gondwana Res.* 100, 87–130. doi:10.1016/j.gr.2021.01.012
- Rudnick, R., and Fountain, D. (1995). Nature and composition of the continental crust—a lower crustal perspective. *Rev. Geophys.* 33, 267–309. doi:10.1029/95rg01302
- Sheir, F., Li, W., Zhang, L., Alabowsh, B., Jiang, L., Liang, L., et al. (2024). Structural geology and chronology of shear zones along the shangdan suture in qinling orogenic belt, China: implications for late mesozoic intra-continental deformation of East asia. *J. Earth Sci.* 35 (2), 376–393. doi:10.1007/s12583-022-1753-7
- Shen, L., Yu, J., O’Reilly, S., Griffin, W., and Zhou, X. (2018). Subduction-related middle permian to early triassic magmatism in central hainan island. *South China* 318, 158–175. (in Chinese with English abstract).
- Song, X., Zhou, M., Can, Z., and Robinson, P. (2004). Late Permian rifting of the South China Craton caused by the Emeishan mantle plume? *J. Geol. Soc.* 161, 773–781. (in Chinese with English abstract).
- Straub, S., Gomez-Tuena, A., Stuart, F., Zellmer, G., Espinasa-Perena, R., Cai, Y., et al. (2011). Formation of hybrid arc andesites beneath thick continental crust. *Earth Planet. Sci. Lett.* 303, 337–347. doi:10.1016/j.epsl.2011.01.013
- Streck, M., Leeman, W., and Chesley, J. (2007). High-magnesian andesite from Mount Shasta: a product of magma mixing and contamination, not a primitive mantle melt. *Geology* 35, 351–354. doi:10.1130/g23286a.1
- Sun, S., and McDonough, W. (1989). “Chemical and isotopic systematics of oceanic basalts: implications for mantle composition and processes”, 42. Geological Society London Special Publications, 313–345. doi:10.1144/gsl.sp.1989.042.01.19
- Tang, H. (1999). Geochemical characteristics of the basalt from chenxing, hainan Island, And their tectonic implication. *Geotect. Metallogenia* 23, 323–327. (in Chinese with English abstract).
- Tatsumi, Y. (2008). Making continental crust: The sanukitoid connection. *Chin. Sci. Bull.* 53, 1620–1633. doi:10.1007/s11434-008-0185-9
- Thieblemont, D., and Tegye, M. (1994). Une discrimination géochimique des roches différenciées témoin de la diversité d’origine et de situation tectonique des magmas calco-alcalins. *Comptes rendus de l’Académie des sciences. Série 2. Sciences de la terre et des planètes* 319, 87–94.
- Wang, C., Wei, C., Yun, P., Lv, C., Lv, Z., and Meng, Z. (2019). Zircon U-Pb age, geochemistry and geological significance of Shunzuo granite in Wuzhishan area, Hainan Island. *Geol. Bull. China* 38, 1352–1361. (in Chinese with English abstract).
- Wang, Y., Lin, W., Faure, M., Van, N., Meng, L., Chu, Y., et al. (2022). Correlation among the Ailaoshan-Song Ma-Song Chay orogenic belts and implications for the evolution of the eastern Paleo-Tethys Ocean. *Tectonophysics* 843, 229618. doi:10.1016/j.tecto.2022.229618
- Wang, Z., Xu, D., Wu, C., Fu, W., Wang, L., and Wu, J. (2013). Discovery of the Late Paleozoic ocean island basalts (OIB) in Hainan Island and their geodynamic implications. *Acta Petrol. Sin.* 29, 875–886. (in Chinese with English abstract).
- Wei, B., Cheng, X., Domeier, M., Zhou, Y., Chen, Q., Jiang, N., et al. (2023). Paleomagnetism of late triassic volcanic rocks from the South qiangtang Block, tibet: constraints on longmuco-shuanghuocean closure in the paleo-tethys realm. *Geophys. Res. Lett.* 50 (19), e2023GL104759. doi:10.1029/2023gl104759
- Winchester, J., and Floyd, P. (1977). Geochemical discrimination of different magma series and their differentiation products using immobile elements. *Chem. Geol.* 20, 325–343. doi:10.1016/0009-2541(77)90057-2
- Xia, B., and Shi, G. (1991). The late palaeozoic rifting in hainan island, China. *Acta Geol. Sin.* 2, 103–115. (in Chinese with English abstract).
- Xu, D., Lin, G., Liang, X., Chen, G., and Tang, H. (2001). The records of the evolution of Precambrian lithosphere: the evidences of petrology and geochemistry of basic rocks on Hainan island. *Acta Petrol. Sin.* 17, 598–608. (in Chinese with English abstract).
- Xu, D., Xia, B., Nonna, B., Ma, C., Li, P., Robert, B., et al. (2006). Characteristics of the Chemdng metabasite massif in Tunchang area, Hainan Island, South China and its tectonic implication. *Acta Petrol. Sin.* 2, 2987–3006. (in Chinese with English abstract).
- Xu, J., Shinjo, R., Defant, M., Wang, Q., and Rapp, R. (2002). Origin of Mesozoic adakitic intrusive rocks in the Ningzhen area of East China: partial melting of delaminated lower continental crust? *Geology* 30, 1111–1114. doi:10.1130/0091-7613(2002)030<1111:oomair>2.0.co;2
- Xu, J., Xia, X., Lai, C., Long, X., and Huang, C. (2019). When did the Paleotethys Ailaoshan Ocean close: new insights from detrital zircon U-Pb age and Hf isotopes. *Tectonics* 38 (5), 1798–1823. doi:10.1029/2018tc005291
- Yu, L., Yan, M., Domeier, M., Guan, C., Shen, M., Fu, Q., et al. (2022). New paleomagnetic and chronological constraints on the Late Triassic position of the eastern Qiangtang terrane: implications for the closure of the paleo-Jinshajiang ocean. *Geophys. Res. Lett.* 49 (2), e2021GL096902. doi:10.1029/2021gl096902
- Zhang, Y., Fu, J., Zhao, Z., Xu, A., Wu, G., and Zeng, B. (1998). Petrographic characteristics and Sm-Nd isotopic dating of the metamorphic basic volcanic rocks in western part of hainan island. *Min. Petr.* 18, 79–84. (in Chinese with English abstract).